THE JOURNAL OF BIOLOGICAL CHEMISTRY VOL. 289, NO. 45, pp. 31111–31120, November 7, 2014


# Increased Spinal Cord $Na^+$-$K^+$-$2Cl^-$ Cotransporter-1 (NKCC1) Activity Contributes to Impairment of Synaptic Inhibition in Paclitaxel-induced Neuropathic Pain*

Received for publication, July 28, 2014, and in revised form, September 15, 2014 Published, JBC Papers in Press, September 24, 2014, DOI 10.1074/jbc.M114.600320

**Shao-Rui Chen**[1], **Lihong Zhu**[1], **Hong Chen, Lei Wen, Geoffroy Laumet, and Hui-Lin Pan**[2]

*From the Center for Neuroscience and Pain Research, Department of Anesthesiology and Perioperative Medicine, The University of Texas MD Anderson Cancer Center, Houston, Texas 77030*

**Background:** Spinal synaptic plasticity may contribute to paclitaxel-induced painful neuropathy.
**Results:** Paclitaxel treatment impairs GABA-mediated neuronal inhibition and increases total and plasma membrane NKCC1 protein levels in the spinal cord. Blocking NKCC1 reverses paclitaxel effects on synaptic inhibition and pain hypersensitivity.
**Conclusion:** Paclitaxel diminishes synaptic inhibition in the spinal cord.
**Significance:** This study demonstrates how disrupting microtubule dynamics causes synaptic plasticity and neuropathic pain.

**Microtubule-stabilizing agents, such as paclitaxel (Taxol), are effective chemotherapy drugs for treating many cancers, and painful neuropathy is a major dose-limiting adverse effect. Cation-chloride cotransporters, such as $Na^+$-$K^+$-$2Cl^-$ cotransporter-1 (NKCC1) and $K^+$-$Cl^-$ cotransporter-2 (KCC2), critically influence spinal synaptic inhibition by regulating intracellular chloride concentrations. Here we show that paclitaxel treatment in rats significantly reduced GABA-induced membrane hyperpolarization and caused a depolarizing shift in GABA reversal potential of dorsal horn neurons. However, paclitaxel had no significant effect on AMPA or NMDA receptor-mediated glutamatergic input from primary afferents to dorsal horn neurons. Paclitaxel treatment significantly increased protein levels, but not mRNA levels, of NKCC1 in spinal cords. Inhibition of NKCC1 with bumetanide reversed the paclitaxel effect on GABA-mediated hyperpolarization and GABA reversal potentials. Also, intrathecal bumetanide significantly attenuated hyperalgesia and allodynia induced by paclitaxel. Co-immunoprecipitation revealed that NKCC1 interacted with β-tubulin and β-actin in spinal cords. Remarkably, paclitaxel increased NKCC1 protein levels at the plasma membrane and reduced NKCC1 levels in the cytosol of spinal cords. In contrast, treatment with an actin-stabilizing agent had no significant effect on NKCC1 protein levels in the plasma membrane or cytosolic fractions of spinal cords. In addition, inhibition of the motor protein dynein blocked paclitaxel-induced subcellular redistribution of NKCC1, whereas inhibition of kinesin-5 mimicked the paclitaxel effect. Our findings suggest that increased NKCC1 activity contributes to diminished spinal synaptic inhibition and neuropathic pain caused by paclitaxel. Paclitaxel disrupts intracellular NKCC1 trafficking by interfering with microtubule dynamics and associated motor proteins.**

Paclitaxel formulated in Cremophor-ethanol (Taxol®) is a first-line chemotherapy drug used to treat many types of cancers, including breast, lung, and ovarian cancers. Neuropathy is a major adverse effect associated with paclitaxel treatment, occurring in as many as 30% of patients (1–3). Symptoms include numbness, tingling, and burning pain. These sensory disorders are often symmetrical and primarily affect distal extremities (4, 5). Paclitaxel-induced neuropathic pain is a major dose-limiting adverse effect, and currently there are no standard treatments to alleviate this debilitating pain.

Microtubules, structures composed of polymerized α- and β-tubulin heterodimers, play fundamental roles in vital cellular processes such as chromosome segregation and intracellular transport (6, 7). Paclitaxel is known to interact within a specific site on β-tubulin of microtubules within the cytoplasm, resulting in microtubule polymerization/stabilization, and leading to disruption of cell division (8, 9). Paclitaxel-induced neuropathy may be caused by dysfunctional microtubules in the dorsal root ganglion (DRG)[3] and peripheral nerves (10). Previous studies have shown that paclitaxel-induced damage to DRG neurons and peripheral nerves (11–13) contributes to painful neuropathy. Although paclitaxel is well known for its effect as a microtubule-stabilizing agent, it is not clear how this action is causally related to neuropathic pain development.

In addition to its accumulation in the peripheral nerves, intermediate concentrations of paclitaxel have been detected in the central nervous system, including the spinal cord, upon systemic administration (14, 15). However, little is known about how paclitaxel affects spinal nociceptive processing or about its role in neuropathic pain. The cation-$Cl^-$ cotransporters,

* This work was supported, in whole or in part, by National Institutes of Health Grant NS073935. This work was also supported by the N. G. and Helen T. Hawkins endowment (to H.-L.P.).
[1] Both authors contributed equally to this work.
[2] To whom correspondence should be addressed: Dept. of Anesthesiology and Perioperative Medicine, Unit 110, The University of Texas MD Anderson Cancer Center, 1515 Holcombe Blvd., Houston, TX 77030-4009. Tel.: 713-563-0822; Fax: 713-794-4590; E-mail: huilinpan@mdanderson.org.

[3] The abbreviations used are: DRG, dorsal root ganglion; AMPAR, AMPA, receptor; EPSC, excitatory postsynaptic current; $E_{GABA}$, reversal potential of GABA-mediated currents; KCC2, $K^+$-$Cl^-$ cotransporter-2; NKCC1, $Na^+$-$K^+$-$2Cl^-$ cotransporter-1; NMDAR, NMDA receptor.

NKCC1 and KCC2, play important roles in balancing intracellular $Cl^-$ concentrations in spinal dorsal horn neurons (16, 17). GABA and glycine are critically involved in regulating nociceptive input in the spinal cord. Activation of $GABA_A$ or glycine receptors opens $Cl^-$ channels and normally inhibits mature neurons in the spinal cord through $Cl^-$ influx to profoundly hyperpolarize dorsal horn neurons because of low intracellular $Cl^-$ concentrations. In this study we determined the potential effects of paclitaxel on synaptic plasticity in the spinal dorsal horn. We provide new evidence that paclitaxel treatment reduces synaptic inhibition and results in a depolarizing shift of GABA reversal potential ($E_{GABA}$) in spinal dorsal horn neurons. This diminished synaptic inhibition by paclitaxel is largely due to increased membrane expression of NKCC1 protein levels in the spinal cord. Blocking NKCC1 normalized synaptic inhibition and pain hypersensitivity induced by paclitaxel. These findings reveal new mechanisms that explain how synaptic plasticity in the spinal cord is involved in the development of chemotherapy-induced neuropathic pain.

## EXPERIMENTAL PROCEDURES

*Animal Model*—Experiments were carried out on adult male rats (Harlan Sprague-Dawley; 220–250 g). The protocols were approved by The University of Texas MD Anderson Cancer Center and were performed in accordance with the National Institutes of Health Guidelines for the Use and Care of Laboratory Animals. To induce painful neuropathy, paclitaxel (2 mg/kg; TEVA Pharmaceuticals) was intraperitoneally injected on four alternate days (1, 3, 5, and 7; with a total cumulative dose of 8 mg/kg) (18). Rats in the control group received intraperitoneal injection of the vehicle (Cremophor EL/ethanol, 1:1) on the same four alternate days. We confirmed the presence of mechanical hyperalgesia and tactile allodynia in the hind paw of rats 10–12 days after paclitaxel treatment. All of the final electrophysiological recordings, behavioral testing, and biochemical experiments were done 2–3 weeks after paclitaxel and vehicle injections.

*Intrathecal Catheter Cannulation*—The rats were anesthetized with 2–3% isoflurane and placed prone on a stereotaxic frame, and a small incision was made at the back of each animal's neck. A PE-10 catheter (8 cm) was inserted via a small opening made in the atlanto-occipital membrane of the cisterna magna such that the caudal tip reached the lumbar spinal enlargement (19). We then exteriorized the rostral end of the catheter and closed the wound with sutures. We allowed the animals to recover for 5–7 days before intrathecal injections.

*Nociceptive Behavioral Tests*—Rats were individually placed on a mesh floor with suspended chambers. After acclimation for 30 min, a series of calibrated von Frey filaments was applied perpendicularly to the plantar surface of both hind paws with sufficient force to bend the filament for 6 s. Brisk withdrawal or paw flinching was considered as a positive response. In the absence of a response, the filament of the next greater force was applied. After a response, the filament of the next lower force was applied. The tactile stimulus producing a 50% likelihood of withdrawal response was calculated by using the "up-down" method (20).

To quantify the mechanical nociceptive threshold, we conducted the paw pressure test on the left hind paw by using the Ugo Basil Analgesiometer. To activate the device, a foot pedal was pressed to activate a motor that applied a constantly increasing force on a linear scale. When the animal displayed pain by either withdrawing of the paw or vocalizing, the pedal was immediately released, and the animal's nociceptive threshold was read on the scale (19).

*Electrophysiological Recordings in Spinal Cord Slices*—The rats were anesthetized with 2–3% isoflurane, and the lumbar spinal cord was quickly removed by using laminectomy. The spinal cord was sectioned (300 $\mu$m thick) with use of a vibrating microtome in ice-cold artificial cerebrospinal fluid solution containing 117 mM NaCl, 3.6 mM KCl, 1.2 mM $MgCl_2$, 2.5 mM $CaCl_2$, 1.2 mM $NaH_2PO_4$, 11 mM glucose, and 25 mM $NaHCO_3$ saturated with 95% $O_2$ and 5% $CO_2$. The slices were preincubated in the artificial cerebrospinal fluid solution at 34 °C for at least 1 h before recording.

We selected lamina II outer neurons for recording because they preferentially receive nociceptive afferent input and are involved in neuropathic pain (21–23). Lamina II neurons were visualized under an upright microscope equipped with epifluorescence and infrared differential interference contrast optics. Conventional whole-cell recordings were conducted to record evoked excitatory postsynaptic currents (EPSCs) and currents elicited by puff application of NMDA or AMPA to spinal lamina II neurons (24). We used a glass pipette (5–10 megaohms) filled with internal solution containing 135 mM potassium gluconate, 5 mM KCl, 2 mM $MgCl_2$, 0.5 mM $CaCl_2$, 5 mM HEPES, 5 mM EGTA, 5 mM ATP-Mg, 0.5 mM Na-GTP, and 10 mM lidocaine *N*-ethyl bromide (adjusted to pH 7.2–7.4 with 1 M KOH; 290–300 millosmoles). The AMPAR-EPSCs were recorded at a holding potential of −60 mV in the presence of 10 $\mu$M bicuculline and 1 $\mu$M strychnine. NMDAR-EPSCs were recorded at +40 mV in the presence of 10 $\mu$M 6-cyano-7-nitroquinoxaline-2,3-dione (CNQX), 10 $\mu$M bicuculline, and 1 $\mu$M strychnine (24). We used electrical stimulation (0.2 ms, 0.6 mA, and 0.1 Hz) of the dorsal root to evoke monosynaptic EPSCs (23, 24). In some neurons, AMPAR currents were elicited in lamina II neurons by puff application of 20 $\mu$M AMPA with use of a positive pressure system (4 p.s.i., 15 ms; Toohey Co., Fairfield, NJ). NMDAR currents were elicited by puff application of 100 $\mu$M NMDA to the recorded neuron at a holding potential of −60 mV (22, 24) by using the pipette internal solution containing 110 mM $Cs_2SO_4$, 2 mM $MgCl_2$, 0.5 mM $CaCl_2$, 5 mM EGTA, 10 mM HEPES, 2 mM MgATP, 10 lidocaine *N*-ethyl bromide, and 0.3 mM $Na_2GTP$ (pH was adjusted to 7.25 with 1 M CsOH; 280–300 millosmoles).

For recording the membrane potential and GABA reversal potential ($E_{GABA}$), we used the $Cl^-$-impermeable gramicidin-perforated patch clamp method (17, 25). The glass pipette solution contained 140 mM CsCl, 5 mM EGTA, and 10 mM HEPES, pH 7.4. Gramicidin was freshly dissolved in DMSO and then diluted into the pipette solution (50 $\mu$g/ml). The neurons were voltage-clamped at −60 mV, and currents that were induced by puff application of GABA (100 $\mu$M) were recorded at various membrane potentials ranging from −90 mV to −30 mV using 10-mV steps in the presence of 1 $\mu$M tetrodotoxin and the $GABA_B$ receptor antagonist CGP55845 (2 $\mu$M). We used

CGP55845 to minimize the confounding effect of $GABA_B$ receptor activation (via G protein-coupled inwardly rectifying $K^+$ channels) on the GABA reversal potential ($E_{GABA}$) and membrane potential during GABA application. The $E_{GABA}$ was determined by using linear regression to calculate a best fit line for the voltage dependence of chloride-mediated currents, and the intercept of the current-voltage line with the abscissa was taken as $E_{GABA}$ (17, 25). In some experiments, the membrane voltage responses of lamina II neurons to GABA (100 $\mu$M) puff application were measured and quantified. The input resistance was monitored, and the recording was abandoned if it changed >15%. All signals were recorded with use of an amplifier (MultiClamp700B; Axon Instruments Inc., Union City, CA), filtered at 1–2 kHz, digitized at 10 kHz, and stored for off-line analysis.

*Quantitative PCR*—Total RNA was extracted by using the TRIzol protocol, reverse-transcribed by using the Superscript III first-strand synthesis kit, and treated with RNase H (Invitrogen). Quantification of NKCC1 mRNA levels was performed by using a SYBR Green PCR kit on an iQ5 real-time PCR detection system (Bio-Rad). The NKCC1 (NM_031798) specific primers used were: 5′-TCAGCCACACTCTCATCAGC-3′ (forward) and 5′-AACCTTTCGCAAACATCTGG-3′ (25). All samples were analyzed in triplicate by using an annealing temperature of 60 °C and normalized by GAPDH (primers: 5′-TGCCACTCAGAAGACTGTGG-3′ and 5′-TTCAGCTCTGGGATGACCTT-3′) expression level. The PCR product specificity was verified by melting-curve analysis and agarose gel electrophoresis.

*Western Immunoblotting*—The lumbar dorsal spinal cord or DRG tissues were homogenized in ice-cold radioimmune precipitation assay buffer containing cocktails of protease and phosphatase inhibitors (Sigma). The homogenate was centrifuged at 12,000 × *g* for 10 min at 4 °C, and the supernatant was collected. The samples were subjected to 12% sodium dodecyl sulfate (SDS)-polyacrylamide gel and transferred to polyvinylidene difluoride membrane. The blots were probed with T4 mouse monoclonal NKCC1 antibody (1:1000; Developmental Studies Hybridoma Bank, University of Iowa, Iowa City, IA) or rabbit anti-KCC2 antibody (N terminus, 1:3000; Santa Cruz Biotechnology, Santa Cruz, CA). An ECL kit (GE Healthcare) was used to detect the protein bands. The amounts of NKCC1 proteins were quantified by normalizing the optical density of their protein band to that of GAPDH in the same samples. The mean values of NKCC1 and KCC2 proteins in control rats were considered to be 1.

In addition, subcellular fractionations of spinal cord tissues were carried out (17, 25) to determine NKCC1 protein levels in the plasma membrane and cytoplasmic fractions. The dorsal quadrants of lumbar spinal cords were homogenized in ice-cold buffer containing 10 mM Tris (pH 7.5), 1 mM EDTA, 1 mM EGTA, 1 mM $Na_3VO_4$, 0.32 M sucrose, and cocktails of protease and phosphatase inhibitors. Homogenate was centrifuged at 1000 × *g* for 10 min at 4 °C to remove nuclei and large debris. The supernatant was then centrifuged at 25,000 × *g* for 30 min at 4 °C to separate the plasma membrane fraction (pellet) and cytoplasmic fraction. The pellet was resuspended in lysis buffer containing 20 mM Tris, pH 7.6, 0.5% Nonidet P-40, 250 mM NaCl, 3 mM EDTA, 3 mM EGTA, 2 mM dithiothreitol, and cocktails of protease and phosphatase inhibitors and sonicated for 5 s at 4 °C.

*Immunoprecipitation*—The immunoprecipitation assay was used to determine whether NKCC1 directly interacts with $\beta$-tubulin or $\beta$-actin in the spinal cord. The dorsal spinal tissues were homogenized in ice-cold lysis buffer and centrifuged at 12,000 × *g* for 10 min at 4 °C. The supernatant was then collected and applied to Dynabeads Protein A that had been pretreated with a mouse NKCC1 antibody overnight at 4 °C. Next, Dynabeads were washed with PBS, 0.5% Tween 20, and the samples were eluted from Dynabeads with use of Tris-glycine SDS sample buffer (Invitrogen) and denatured at 70 °C for 10 min before gel electrophoresis. The protein concentration was quantified by using the Lowry protein assay. For immunoblots, lysates were separated by 4–12% gradient SDS-polyacrylamide gel and transferred to a polyvinylidene fluoride membrane. We then probed the blots with a rabbit anti-$\beta$-tubulin antibody (1:5000) or a rabbit anti-$\beta$-actin antibody (1:2000, Abcam). Immunoblots were then developed with an enhanced ECL kit.

*Drugs and Chemicals*—Bumetanide was purchased from Sigma. Ciliobrevin D and jasplakinolide were obtained from EMD Millipore (Billerica, MA). Ispinesib was purchased from Selleckchem (Houston, TX). The effective concentrations of these inhibitors and the paclitaxel used in the *in vitro* experiments had been demonstrated in previous studies (25–30).

*Statistical Analysis*—Data were presented as the means ± S.E. To compare the difference in the electrophysiological and biochemical data between paclitaxel-treated and vehicle-treated control groups, we used paired Student's *t* test or repeated measures of analysis of variance followed by Tukey's post hoc test. To determine the effect of bumetanide on the paw withdrawal thresholds and the effect of drug treatments on NKCC1 protein levels in spinal cord slices, repeated measures of analysis of variance followed by Dunnett's post hoc test were used. We used corresponding nonparametric analysis (*i.e.* Mann-Whitney or Kruskal-Wallis test) when data were not normally distributed. The level of statistical significance was set at $p < 0.05$.

## RESULTS

*Paclitaxel Treatment Impairs Synaptic Inhibition and Causes a Depolarizing Shift in $E_{GABA}$ in the Spinal Dorsal Horn*—GABA- and glycine-mediated synaptic inhibition in the spinal cord dorsal horn is critically involved in modulation of nociceptive input from primary afferent nerves (16, 17). To determine whether systemic paclitaxel treatment changes synaptic inhibition in the spinal dorsal horn, we first recorded membrane potential responses of puff application of GABA directly to lamina II neurons (17). In neurons recorded from vehicle-treated control rats, puff application of GABA caused a large hyperpolarization of the membrane potential. The GABA-induced neuronal hyperpolarization was significantly smaller in paclitaxel-treated rats than in vehicle-treated control rats (Fig. 1, *A* and *B*).

We next determined whether reduced GABAergic inhibition of spinal dorsal horn neurons in paclitaxel-treated rats is associated with changes in GABA reversal potential ($E_{GABA}$), which reflects intracellular chloride levels (16, 17, 31). In lamina II

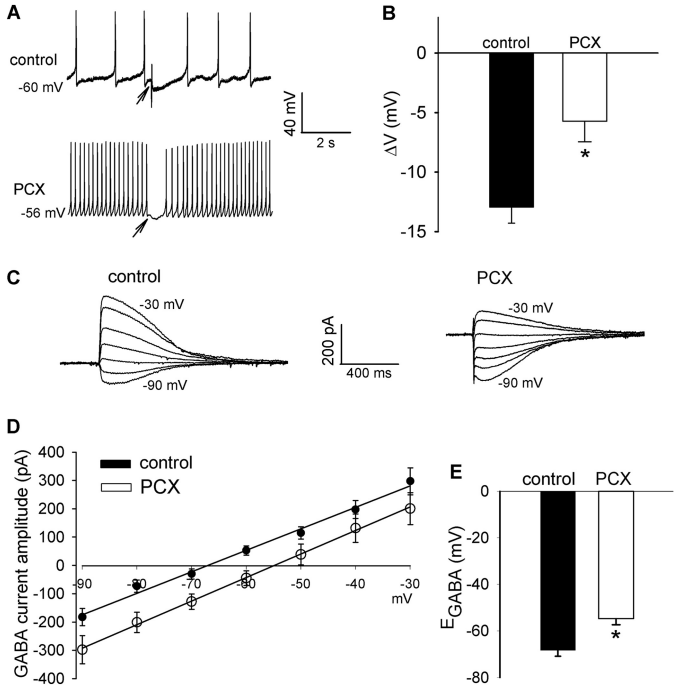


FIGURE 1. **Paclitaxel treatment diminishes GABA-mediated synaptic inhibition and causes a depolarizing shift in $E_{GABA}$ in spinal dorsal horn neurons.** *A* and *B*, representative perforated recordings and mean data show changes in membrane potentials in response to puff application of 100 $\mu$M GABA to lamina II neurons in vehicle-treated control and paclitaxel (*PCX*)-treated rats ($n$ = 16 and 18 neurons, respectively). *Arrows* indicate the time when GABA was puffed to the neuron. *C* and *D*, original current traces and mean current-voltage plot data show the GABA-elicited currents recorded at different holding potentials in lamina II neurons from vehicle-treated control and paclitaxel-treated rats ($n$ = 18 and 19 neurons, respectively). *E*, mean data show the difference in the GABA reversal potentials of lamina II neurons recorded in *D*. *, $p < 0.05$ compared with the control group. *Error bars* represent the S.E.

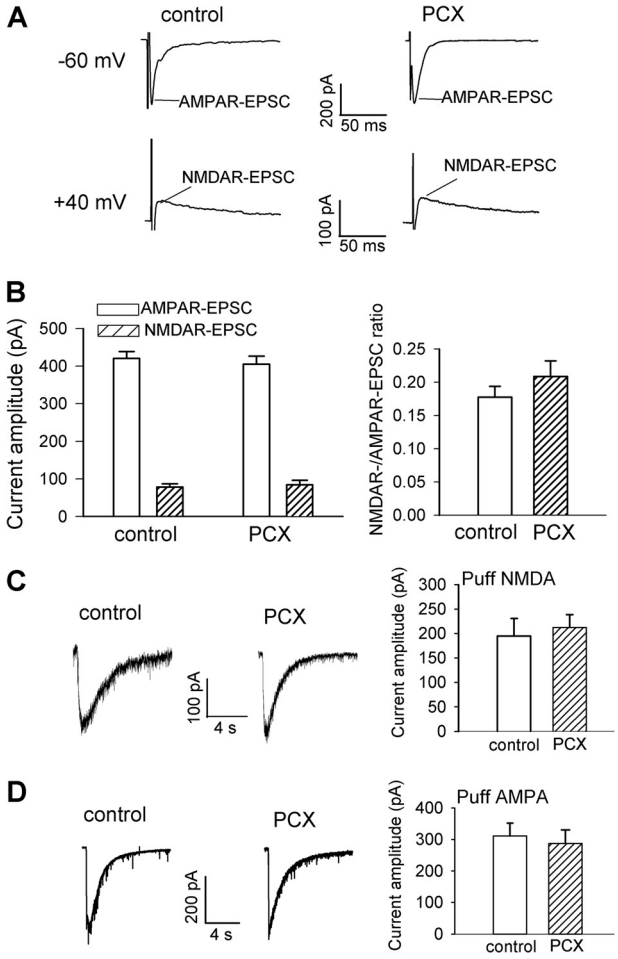


FIGURE 2. **Paclitaxel treatment does not significantly alter AMPAR and NMDAR activities of spinal dorsal horn neurons.** *A* and *B*, original current traces and mean data show the amplitude and ratio of evoked NMDAR-EPSCs to AMPAR-EPSCs of lamina II neurons recorded from vehicle-treated control and paclitaxel (*PCX*)-treated rats ($n$ = 19 neurons in each group). The holding potential for recording AMPAR-EPSCs and NMDAR-EPSCs is indicated on the *left*. *C*, representative traces and mean data of the amplitude of NMDAR currents elicited by puff application of 100 $\mu$M NMDA to lamina II neurons recorded from vehicle-treated control and paclitaxel-treated rats ($n$ = 11 and 12 neurons, respectively). *D*, representative traces and mean data of the amplitude of AMPAR currents elicited by puff application of 20 $\mu$M AMPA to lamina II neurons recorded from vehicle-treated control and paclitaxel-treated rats ($n$ = 12 neurons in each group). *Error bars* represent the S.E.

neurons recorded from control rats, the $E_{GABA}$ was ~−70 mV. In paclitaxel-treated rats there was a significant depolarizing shift (~14 mV) in $E_{GABA}$ of lamina II neurons (Fig. 1, *C–E*). These results suggest that paclitaxel treatment diminishes synaptic inhibition by interrupting chloride homeostasis in the spinal dorsal horn.

*Paclitaxel Treatment Does Not Alter AMPAR- and NMDAR-mediated Glutamatergic Input in the Spinal Dorsal Horn*—Glutamate is the principal excitatory neurotransmitter involved in synaptic transmission through activation of AMPARs and NMDARs. Increased glutamatergic input to spinal cord second-order sensory neurons is involved in nerve injury-induced neuropathic pain (24). We have shown that increased NMDAR activity by nerve injury can impair synaptic inhibition through calcium- and calpain-mediated KCC2 proteolysis in the spinal cord (17). To determine whether paclitaxel alters the activity of AMPARs and NMDARs in the spinal dorsal horn, we first recorded AMPAR-EPSCs and NMDAR-EPSCs of lamina II neurons monosynaptically evoked by electrical stimulation of the attached dorsal root in spinal cord slices. The amplitudes of AMPAR-EPSCs and NMDAR-EPSCs evoked from the dorsal root did not differ significantly between vehicle-treated control rats and paclitaxel-treated rats (Fig. 2, *A* and *B*). Also, the ratio of NMDAR-EPSCs to AMPAR-EPSCs of lamina II neurons was similar in vehicle-treated control and paclitaxel-treated rats (Fig. 2*B*).

To specifically determine the effect of paclitaxel treatment on the activity of postsynaptic AMPARs and NMDARs in the spinal dorsal horn, we examined the currents elicited by direct puff application of AMPA (20 $\mu$M) or NMDA (100 $\mu$M) to recorded lamina II neurons (22, 24). The amplitudes of AMPA- and NMDA-elicited currents of lamina II neurons did not differ significantly between vehicle-treated control rats and paclitaxel-treated rats (Fig. 2, *C* and *D*). These results suggest that paclitaxel-induced impairment of synaptic inhibition is not associated with increased glutamatergic input in the spinal dorsal horn.

*Paclitaxel Treatment Increases NKCC1 Protein Levels in the Spinal Cord*—Both NKCC1 and KCC2 are crucially involved in regulating intracellular $Cl^-$ levels in the spinal cord (17, 32). To determine whether paclitaxel affects the expression level of

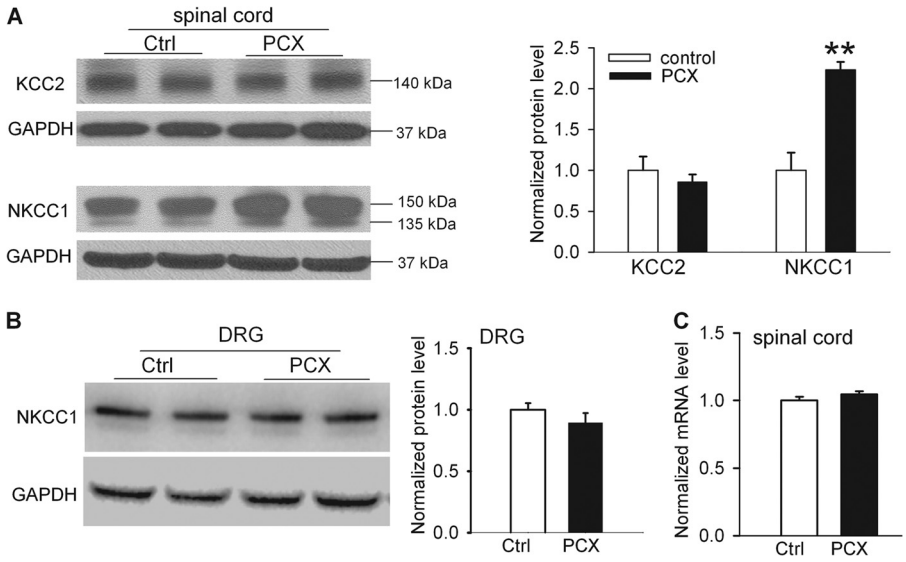


FIGURE 3. **Paclitaxel treatment increases NKCC1, but not KCC2, protein levels in the spinal cords.** *A*, original gel images (*left*) and quantification (*right*) of KCC2 (~140 kDa) and NKCC1(~150 kDa and 135 kDa) in the dorsal spinal cord from vehicle-treated control and paclitaxel (*PCX*)-treated rats ($n = 8$ rats in each group). *B*, original gel blots (*left*) and quantification (*right*) of protein levels of NKCC1 in the DRG from vehicle-treated control and paclitaxel-treated rats ($n = 6$ rats in each group). GAPDH in the same sample was used as a loading control. *C*, mean data show the NKCC1 mRNA level in the dorsal spinal cord from vehicle-treated control and paclitaxel-treated rats ($n = 8$ rats in each group). **, $p < 0.01$ compared with the control group. *Error bars* represent the S.E.

NKCC1 and KCC2 in the spinal cord, we used Western blotting to measure the protein levels of NKCC1 and KCC2 in the lumbar spinal cord removed from paclitaxel- and vehicle-treated rats. We detected two NKCC1 protein bands (~150 and ~135 kDa) in the dorsal spinal cord. The lower protein band of NKCC1 (~135 kDa) seemed to be a degradation product because it disappears in the NKCC1-null mouse (33). The NKCC1 protein level in the dorsal spinal cord was substantially higher in paclitaxel-treated rats than in control rats (Fig. 3*A*). However, there was no significant difference in the KCC2 protein level (~140 kDa) in dorsal spinal cords between paclitaxel-treated and vehicle-treated rats (Fig. 3*A*).

We next quantified the protein level of NKCC1 in the lumbar DRGs. The protein level of NKCC1 in the DRG did not differ significantly between paclitaxel-treated and vehicle-treated rats (Fig. 3*B*). Also, we used real-time PCR to determine whether paclitaxel treatment increases NKCC1 transcriptional expression in the spinal cord. The mRNA level of NKCC1 in the dorsal spinal cord in paclitaxel-treated rats was similar to that in control rats (Fig. 3*C*). Together, these data indicate that paclitaxel treatment increases the NKCC1 protein level, but not its transcriptional expression, in the spinal cord.

*Increased NKCC1 Activity Mediates Impaired Synaptic Inhibition and $E_{GABA}$ Shift in the Spinal Cord Caused by Paclitaxel*—We next determined whether increased NKCC1 protein levels contribute to reduced synaptic inhibition and $E_{GABA}$ shift induced by paclitaxel treatment using 20 $\mu$M bumetanide, a selective NKCC1 inhibitor (25, 31). Although bumetanide has a similar potency of inhibiting NKCC1 and NKCC2 (34), NKCC2 is not expressed in the spinal cord or DRG (35, 36). Also, bumetanide does not inhibit KCC2 unless it is used at very high concentrations (500–1000 $\mu$M) (37, 38). Incubating the spinal cord slices with 20 $\mu$M bumetanide for 2–3 h completely normalized the depolarizing shift in the $E_{GABA}$ of lamina II neurons from paclitaxel-treated rats (Fig. 4, *A*–*C*). Also, bumetanide treatment restored the level of GABA-mediated membrane hyperpolarization of lamina II neurons from paclitaxel-treated rats (Fig. 4, *D* and *E*). However, bumetanide treatment had no significant effect on GABA-induced membrane hyperpolarization or $E_{GABA}$ of lamina II neurons from control rats (Fig. 4 *versus* Fig. 1). These results suggest that increased NKCC1 activity contributes to impaired synaptic inhibition of spinal dorsal horn neurons induced by paclitaxel.

*Increased NKCC1 Activity at the Spinal Level Contributes to Pain Hypersensitivity Caused by Paclitaxel*—We also determined whether increased NKCC1 activity at the spinal level is involved in paclitaxel-induced pain hypersensitivity in rats. Bumetanide was dissolved in vehicle (DMSO) and administered intrathecally in a volume of 5 $\mu$l followed by a 10-$\mu$l flush with normal saline. Intrathecal injection of DMSO had no significant effects on allodynia or mechanical hyperalgesia in all rats tested. Intrathecal injection of 2.5–20 ng of bumetanide significantly reduced tactile allodynia and mechanical hyperalgesia in paclitaxel-treated rats in a dose-dependent manner ($n = 12$ rats in each group; Fig. 5). The effect of bumetanide was observed 30 min after a single injection and lasted about 90 min. These data suggest that increased NKCC1 activity at the spinal level contributes to paclitaxel-induced neuropathic pain.

*Systemic Paclitaxel Treatment Increases NKCC1 Protein Levels at Plasma Membranes in the Spinal Cord*—Because paclitaxel treatment increased the total NKCC1 protein level in the spinal cord and because the NKCC1 activity is largely determined by its protein level at the plasma membrane (32), we investigated whether systemic paclitaxel treatment alters the NKCC1 protein distribution in the plasma membrane and cytosolic fractions. In paclitaxel-treated rats, the NKCC1 protein level in the plasma membrane fraction of dorsal spinal cords was significantly increased compared with that in control rats (Fig. 6, *A* and *B*). Furthermore, the NKCC1 protein level in dorsal spinal cords in the cytosolic fraction was significantly

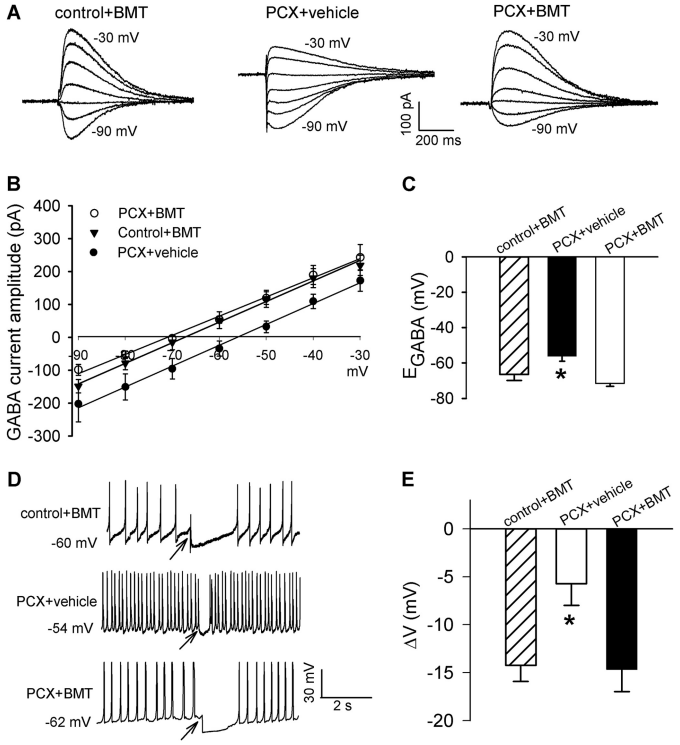


FIGURE 4. **NKCC1 inhibition restores the level of GABA-mediated synaptic inhibition in spinal cords of paclitaxel-treated rats.** *A* and *B*, representative traces of GABA-induced currents recorded at different holding potentials and mean current-voltage plot data show the GABA reversal potentials of lamina II neurons from spinal cords of control rats pretreated with 20 $\mu$M bumetanide (*BMT*) and spinal cords of paclitaxel (*PCX*)-treated rats pretreated with vehicle (0.02% DMSO) or 20 $\mu$M bumetanide ($n$ = 14, 12, and 18 neurons, respectively). *C*, mean data show the difference in the GABA reversal potentials of the same neurons recorded in *B*. *D* and *E*, original perforated recordings and mean data show changes in membrane potentials in response to puff application of 100 $\mu$M GABA to lamina II neurons in the spinal cords of control rats pretreated with bumetanide and spinal cords of paclitaxel-treated rats pretreated with vehicle (0.02% DMSO) or bumetanide ($n$ = 14, 14, and 15 neurons in each group). *Arrows* indicate the time when GABA was puffed to the neuron. *, $p < 0.05$ compared with the control group. *Error bars* represent the S.E.

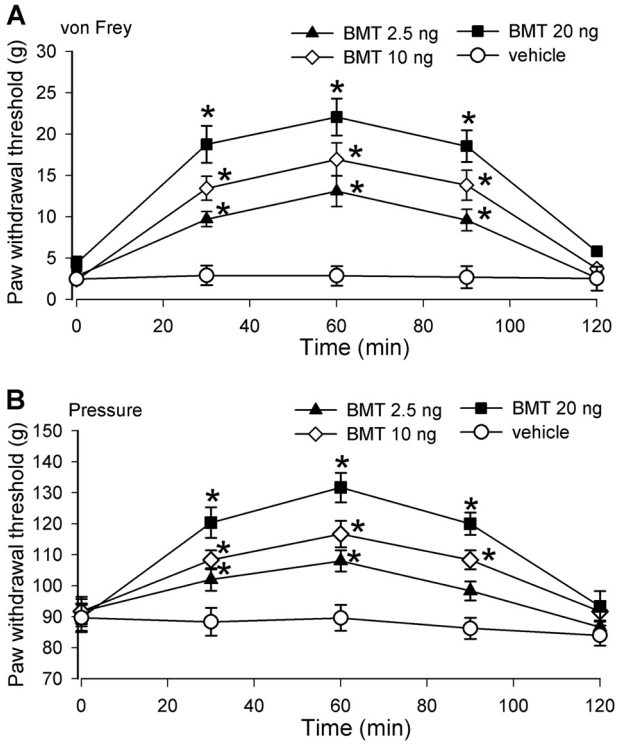


FIGURE 5. **Inhibition of NKCC1 at the spinal level attenuates pain hypersensitivity of paclitaxel-treated rats.** *A* and *B*, time course of the mean effects of intrathecal injection of bumetanide or vehicle on tactile allodynia (*A*) and mechanical hyperalgesia (*B*) of paclitaxel-treated rats. Bumetanide (*BMT*; 2.5, 10, and 20 ng; $n$ = 10 rats in each group) or vehicle (0.1% DMSO, $n$ = 7 rats) was administered in rats 12–15 days after paclitaxel treatment. *, $p <$ 0.05 compared with respective baseline control (time 0). *Error bars* represent the S.E.

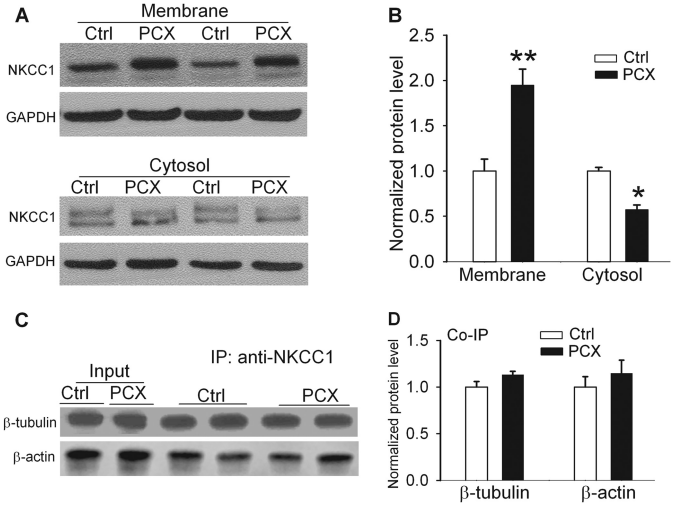


FIGURE 6. **Effects of systemic paclitaxel treatment on NKCC1 subcellular redistribution and association of NKCC1 with microtubules in the spinal cord.** *A* and *B*, original gel blots and quantification of NKCC1 protein levels in the plasma membrane and cytosolic fractions of spinal cords obtained from vehicle-treated control and paclitaxel (*PCX*)-treated rats ($n$ = 8 rats in each group). *C* and *D*, original gel images and quantification of protein levels of $\beta$-tubulin and $\beta$-actin in the NKCC1 immunoprecipitates (*IP*) of spinal cords obtained from vehicle-treated control and paclitaxel-treated rats ($n$ = 6 rats in each group). *, $p < 0.05$; **, $p < 0.01$ compared with the control group. *Error bars* represent the S.E.

lower in paclitaxel-treated than in vehicle-treated rats (Fig. 6, *A* and *B*).

*Association of NKCC1 with Microtubules in the Spinal Cord*—Microtubules, formed by the polymerization of a dimer of two globular proteins, $\alpha$- and $\beta$-tubulin, are highly dynamic (7). They provide platforms for intracellular transport, including the movement of secretory vesicles, organelles, and intracellular substances. We performed co-immunoprecipitation experiments to determine whether NKCC1 directly interacts with $\beta$-tubulin and whether paclitaxel alters the association of NKCC1 and $\beta$-tubulin. Proteins extracted from the dorsal spinal cords were first immunoprecipitated with an NKCC1 antibody and then blotted with a $\beta$-tubulin or a $\beta$-actin antibody. Both $\beta$-tubulin and $\beta$-actin proteins were readily detected in the spinal immunoprecipitates (Fig. 6, *C* and *D*). Also, the $\beta$-tubulin and $\beta$-actin protein levels in the NKCC1 immunoprecipitates did not differ significantly between paclitaxel-treated and vehicle-treated rats (Fig. 6, *C* and *D*). Thus, although NKCC1 directly interacts with $\beta$-tubulin and $\beta$-actin in the spinal cord, it seems that paclitaxel-induced increases in NKCC1 protein levels are not due to increased NKCC1 binding to microtubules.

*Paclitaxel Induces NKCC1 Subcellular Redistribution in the Spinal Cord by Interfering with Microtubules*—We next determined whether direct treatment of spinal cord tissues with

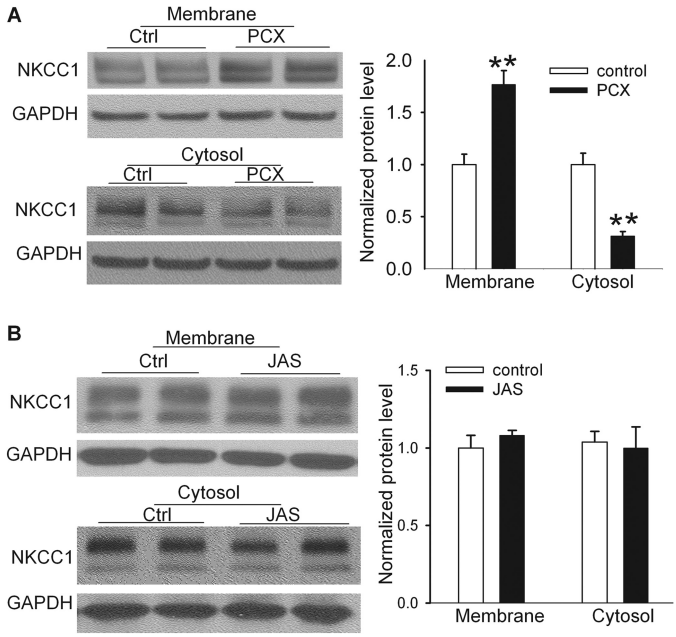


FIGURE 7. **Paclitaxel causes NKCC1 subcellular redistribution in the spinal cord through stabilizing microtubules but not actin.** *A*, original blot images and quantification of NKCC1 protein levels in the plasma membrane and cytosolic fractions of spinal cord slices treated with vehicle (*Ctrl*, Cremophor EL/ethanol 1:1; $n = 8$ rats) or paclitaxel (*PCX*, 10 $\mu$M, $n = 8$ rats) for 3 h. *B*, original gel images and quantification of NKCC1 protein levels in the plasma membrane and cytosolic fractions of spinal cord slices treated with vehicle control (0.1% DMSO, $n = 6$ rats) or jasplakinolide (*JAS*, 125 nM, $n = 6$ rats) for 3 h. **, $p < 0.01$ compared with the control group. *Error bars* represent the S.E.

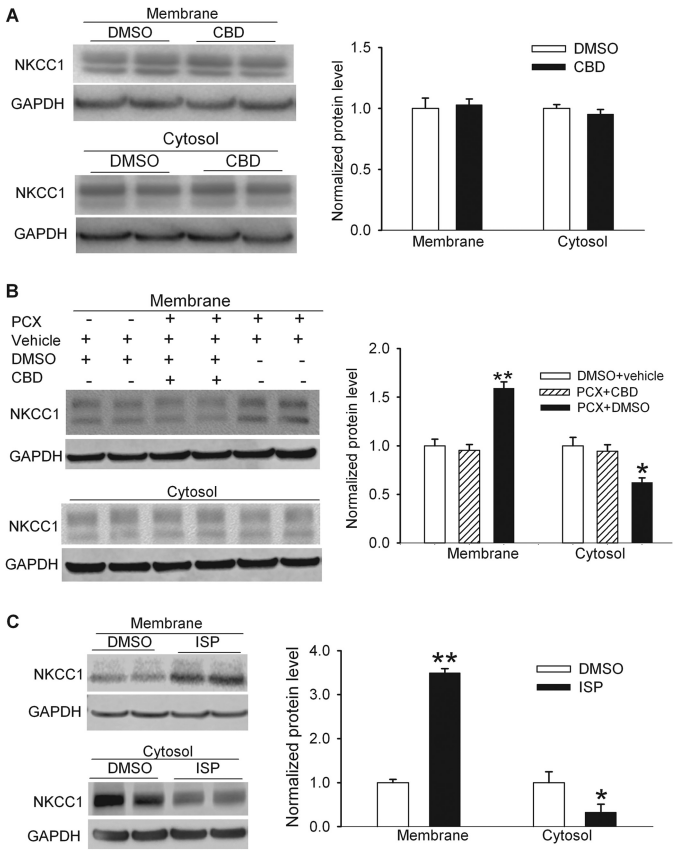


FIGURE 8. **Paclitaxel causes NKCC1 subcellular redistribution in the spinal cord through increased dynein activity.** *A*, original blot images and quantification of NKCC1 protein levels in the plasma membrane and cytosolic fractions of spinal cord slices treated with vehicle (*Ctrl*, 0.1% DMSO) or ciliobrevin D (*CBD*, 50 $\mu$M) for 3 h. $n = 6$ rats in each group. *B*, original gel images and quantification of NKCC1 protein levels in the plasma membrane and cytosolic fractions of spinal cord slices treated with DMSO plus vehicle (Cremophor EL/ethanol), paclitaxel (*PCX*, 10 $\mu$M) plus ciliobrevin D, or PCX plus DMSO for 3 h. $n = 6$ rats in each group. *C*, original blot images and quantification of NKCC1 protein levels in the plasma membrane and cytosolic fractions of spinal cord slices with vehicle (*Ctrl*, 0.1% DMSO) or ispinesib (*ISP*, 1 $\mu$M). * $p < 0.05$; ** $p < 0.01$, compared with the vehicle control group. *Error bars* represent the S.E.

paclitaxel induces a similar subcellular redistribution of NKCC1 proteins. For this experiment, we first prepared the dorsal spinal cord slices (400 $\mu$m) using a vibratome and treated the slices with 10 $\mu$M paclitaxel (26) or vehicle (Cremophor EL/ethanol) for 3 h. We then collected the spinal cord slices and extracted proteins from the plasma membrane and cytosolic fractions. Remarkably, incubation of spinal cord slices with paclitaxel *in vitro* significantly increased the NKCC1 protein level in the plasma membrane accompanied by a reduction in the NKCC1 protein level in the cytosolic fraction in the spinal cord (Fig. 7*A*).

Because actin is another critical cytoskeletal protein involved in the vesicle and organelle movement inside a cell, we determined whether stabilizing actin also can affect NKCC1 subcellular redistribution in the spinal cord. We incubated the spinal cord slices with vehicle (DMSO) or 125 nM jasplakinolide for 3 h. Jasplakinolide is a cyclo-depsipeptide and specific actin stabilizer that can enhance actin polymerization (27, 39, 40) and prevent disassembly of actin filaments (28). There were no differences in the NKCC1 protein levels in the plasma membrane or cytosolic fractions between jasplakinolide-treated and vehicle-treated spinal cord tissues (Fig. 7*B*). These results indicate that paclitaxel increases NKCC1 protein abundance in the plasma membranes of the spinal cord by interrupting microtubule dynamics.

*Paclitaxel Induces NKCC1 Subcellular Redistribution in the Spinal Cord through Dynein Activation*—Cytoplasmic dynein is a multisubunit, microtubule-associated, force-producing enzyme that is required for various intracellular transport processes, including the endocytic pathway, transport of organelles, and microtubule-dependent mitotic processes (6, 41). Increased microtubule polymerization by paclitaxel can increase the dynein activity through elevated intracellular calcium concentrations (42, 43). To determine whether dynein activation is involved in paclitaxel-induced cellular redistribution of NKCC1 in the spinal cord, we treated the spinal cord slices with 10 $\mu$M paclitaxel in the presence of 50 $\mu$M ciliobrevin D or its vehicle (DMSO) for 3 h. Ciliobrevin D is a specific membrane-permeable dynein inhibitor (29). Treatment with ciliobrevin D alone had no significant effect on the NKCC1 protein levels in the plasma membrane or cytosolic fractions (Fig. 8*A*). In the presence of ciliobrevin D, paclitaxel failed to significantly alter the NKCC1 protein levels in the plasma membrane or cytosolic fractions (Fig. 8*B*). These data suggest that increased dynein activity by paclitaxel-induced microtubule polymerization contributes to increased NKCC1 protein levels at the plasma membranes in the spinal cord.

*Blocking Kinesin-5 Mimics the Paclitaxel Effect on Subcellular NKCC1 Distribution in the Spinal Cord*—Kinesin-5, also termed KIF11, kinesin spindle protein, or Eg5, is another major

microtubule motor protein. Among nondividing cells, kinesin-5 is most enriched within neurons (44, 45) and can restrict the movement of short microtubules in dendrites (46). Because kinesin-5 has an opposite action of dynein on intracellular trafficking (45–47), we determined whether inhibition of kinesin-5 mimics the paclitaxel effect on the subcellular redistribution of NKCC1 in the spinal cord. Ispinesib is a potent and specific inhibitor of kinesin-5 (30). We treated the dorsal spinal cord slices with 1 $\mu$M ispinesib or vehicle for 3 h. Treatment with ispinesib significantly increased the NKCC1 protein levels in the plasma membrane fraction and reduced the NKCC1 protein levels in the cytosolic fraction (Fig. 8*C*). These results suggest that the basal activity of kinesin-5 is actively involved in increased NKCC1 trafficking in the spinal cord.

## DISCUSSION

Our study provides new evidence that diminished synaptic inhibition due to an increase in NKCC1 activity in the spinal dorsal horn is involved in paclitaxel-induced neuropathic pain. $GABA_A$ or glycine receptor-mediated synaptic inhibition of spinal dorsal horn neurons normally attenuates nociceptive transmission by reducing the impact of action potentials coming from primary afferent nerves (16, 17). A major finding of our study is that the membrane hyperpolarization of spinal dorsal horn neurons produced by GABA was much less in paclitaxel-treated rats than in vehicle-treated control rats. Also, paclitaxel treatment caused a significant depolarizing shift of $E_{GABA}$ in spinal dorsal horn neurons. These data suggest that paclitaxel reduces synaptic inhibition in the spinal dorsal horn, which links impaired microtubule dynamics to synaptic plasticity in paclitaxel-induced painful neuropathy.

The cation chloride cotransporters NKCC1 and KCC2 regulate intracellular $Cl^-$ concentrations and determine the physiological actions of $GABA_A$ and glycine receptor activation. The direction and degree of $GABA_A$ or glycine receptor-mediated $Cl^-$ currents in neurons depend, among other factors, on the $Cl^-$ gradient across the plasma membrane, which in turn depends on the relative activity of NKCC1 (raising intracellular $Cl^-$) and KCC2 (lowering intracellular $Cl^-$) (16, 17, 31). Accordingly, increased NKCC1 activity reduces synaptic inhibition, whereas increased KCC2 activity has an inverse effect, enhancing synaptic inhibition. Traumatic nerve injury increases NMDAR activity of spinal dorsal horn neurons and impairs synaptic inhibition through calpain-mediated KCC2 protein degradation (17). However, in this study we found that paclitaxel treatment had no significant effect on the NMDAR activity in the spinal dorsal horn. Consistent with our findings, it has been reported that paclitaxel application does not affect NMDAR activity of hippocampal neurons (48). Because paclitaxel treatment had no significant effect on NMDAR activity or KCC2 protein levels in the spinal cord, our findings reinforce the notion that different neuropathic pain conditions do not share the same cellular and molecular mechanisms (24). Interestingly, we found that paclitaxel treatment caused a large increase in NKCC1 protein levels in the spinal cord. However, paclitaxel did not significantly alter the mRNA level of NKCC1 in the spinal cord, suggesting that NKCC1 up-regulation is not due to increased transcription. It is possible that stabilizing microtubules by paclitaxel may cause NKCC1 protein accumulation in the spinal cord. Cell surface proteins including NKCC1 undergo endocytosis and trafficking to lysosomes for degradation (49). Microtubules are closely associated with lysosomes and play a major role in intracellular transport of lysosomes inside cells (50). NKCC1 is colocalized with markers of early and recycling endosomes, implicating endocytic recycling in cell-specific anion transport (51). Because translocation of endosomes and lysosomes occurs along microtubules (52), disruption of endocytic events by paclitaxel may cause accumulation of NKCC1 proteins in the spinal cord. Also, it is possible that increased protein translation by paclitaxel may contribute increased NKCC1 protein levels in the spinal cord.

Another salient finding of our study is that paclitaxel treatment causes subcellular redistribution of NKCC1 proteins in the spinal cord. Paclitaxel specifically binds to the inner surface of $\beta$-tubulin along the length of microtubules (9). Microtubules in the neuron undergo dynamic assembly and disassembly, bundling and splaying, and rapid transport as well as integration with other cytoskeletal elements such as actin filaments (53, 54). These various behaviors are regulated by signaling pathways that affect microtubule-related proteins such as molecular motor proteins. In neurons treated with paclitaxel, the density of microtubules increases, and the normal domain structure of individual microtubules is lost because the microtubules are stabilized all along their lengths and flaws arise in the normal polarity patterns of the microtubules (6). Our co-immunoprecipitation experiments indicate that NKCC1 and $\beta$-tubulin form a protein complex in the spinal cord. We found unexpectedly that *in vivo* or *in vitro* paclitaxel treatment significantly increased NKCC1 enrichment at the plasma membrane but reduced the NKCC1 protein level in the cytosolic fraction. In contrast, we found that promoting actin polymerizing and stabilizing by jasplakinolide had no significant effect on the subcellular redistribution of NKCC1 in the spinal cord. Thus, paclitaxel-induced increases in the membrane NKCC1 protein levels are predominantly dependent on microtubule dynamics.

Our findings suggest that increased NKCC1 surface expression and activity in the spinal cord contribute to paclitaxel-induced impairment of synaptic inhibition and pain hypersensitivity. Increased NKCC1 translocation to the plasma membrane and increased NKCC1 activity probably contribute to diminished synaptic inhibition because of an increase in intracellular $Cl^-$ accumulation. In support of this hypothesis, we found that inhibition of NKCC1 with bumetanide normalized the level of GABA-induced membrane hyperpolarization and restored $E_{GABA}$ of spinal dorsal horn neurons in paclitaxel-treated rats. In addition, we showed that intrathecal treatment with bumetanide significantly attenuated allodynia and hyperalgesia caused by paclitaxel. We observed that paclitaxel increased the plasma membrane NKCC1 levels within 3 h in spinal cord slices. However, pain hypersensitivity induced by paclitaxel typically takes 1–3 days to develop in this rat model. This mismatch in the time course could be explained by the fact that many different factors and mechanisms contribute to the development of pain after paclitaxel treatment. Because increased NKCC1 activity primarily reduces synaptic inhibition, this mechanism alone may not adequately account for the

time course of paclitaxel-induced pain. Thus, paclitaxel-induced pain hypersensitivity is probably caused by a gradual increase in abnormal discharge activity from damaged primary afferent nerves (11, 13) and the concurrent loss of spinal synaptic inhibition, which potentiates nociceptive input to dorsal horn neuron.

Motor proteins are the driving force behind most active transport of proteins and vesicles in the cytoplasm. Microtubule motors, including cytoplasmic dynein and kinesin-5, move along microtubules by interacting with tubulins (47, 55–57). There are two basic types of microtubule motors: plus-end motors and minus-end motors, depending on the direction in which they move along the microtubule track within the cell. Dyneins typically walk along microtubules toward the minus end, whereas kinesins mainly walk along microtubules toward the plus end (6, 7, 47). Cytoplasmic dynein can generate a discrete power stroke as well as a possessive walk in either direction, *i.e.* toward the plus or minus end of a microtubule (58). Stabilizing microtubules with paclitaxel can stimulate dynein activity via increased intracellular calcium levels (42, 43). It has been shown that dynein is actively involved in the membrane surface expression of $K^+$ channels (41, 59). In this study we found that inhibition of dynein activity blocked the effect of paclitaxel on the subcellular redistribution of NKCC1 in the spinal cord, suggesting that increased dynein activation by paclitaxel is involved in increased NKCC1 membrane trafficking.

On the other hand, we found that inhibition of kinesin-5 mimicked the effect of paclitaxel on subcellular redistribution of NKCC1 in the spinal cord, suggesting that kinesin-5 is actively involved in endocytotic movement of NKCC1 in spinal dorsal horn neurons. Kinesin-5 is a slow motor compared with cytoplasmic dynein and can act as a "brake" to modulate the activity of dynein (60). Depletion or inhibition of kinesin-5 from cultured neurons results in an axon that grows faster (45–47), which could be explained by the kinesin-5 capacity to oppose cytoplasmic dynein. Collectively, our findings suggest that motor proteins are important for regulating NKCC1 trafficking by interacting with microtubules in the spinal cord. However, the precise mechanisms as to how dynein and kinesin-5 interact with microtubules to regulate intracellular NKCC1 movement remain poorly understood. Further studies are warranted to delineate the complex mechanisms involved in dynein- and kinesin-associated NKCC1 transport in the spinal cord, the paclitaxel effects on NKCC1 distribution in endosomes and lysosomes inside neurons, and the signaling pathways involved in motor protein-dependent NKCC1 targeting in the plasma membrane and cytosol.

To conclude, our study provides new information about the involvement of synaptic plasticity in the spinal cord in paclitaxel-induced neuropathic pain. Paclitaxel treatment increases NKCC1 activity and the NKCC1 protein level in the plasma membrane in the spinal cord. The motor protein dynein is involved in paclitaxel-induced subcellular NKCC1 redistribution in the spinal cord. Increased spinal NKCC1 activity contributes to disruption of $Cl^-$ homeostasis, diminished synaptic inhibition, and pain hypersensitivity caused by paclitaxel. Therefore, reducing NKCC1 activity could represent a new strategy for restoring spinal synaptic inhibition to treat chemotherapy-induced neuropathic pain.

## REFERENCES


1. Grisold, W., Cavaletti, G., and Windebank, A. J. (2006) Peripheral neuropathies from chemotherapeutics and targeted agents: diagnosis, treatment, and prevention. *Neurol. Oncol.* **14,** 45–54
2. Lee, J. J., and Swain, S. M. (2006) Peripheral neuropathy induced by microtubule-stabilizing agents. *J. Clin. Oncol.* **24,** 1633–1642
3. Scripture, C. D., Figg, W. D., and Sparreboom, A. (2006) Peripheral neuropathy induced by paclitaxel: recent insights and future perspectives. *Curr. Neuropharmacol.* **4,** 165–172
4. Rowinsky, E. K., Chaudhry, V., Cornblath, D. R., and Donehower, R. C. (1993) Neurotoxicity of Taxol. *J. Natl. Cancer Inst. Monogr.* **15,** 107–115
5. Polomano, R. C., and Bennett, G. J. (2001) Chemotherapy-evoked painful peripheral neuropathy. *Pain Med.* **2,** 8–14
6. Baas, P. W., and Ahmad, F. J. (2013) Beyond taxol: microtubule-based treatment of disease and injury of the nervous system. *Brain* **136,** 2937–2951
7. Conde, C., and Cáceres, A. (2009) Microtubule assembly, organization and dynamics in axons and dendrites. *Nat. Rev. Neurosci.* **10,** 319–332
8. De Brabander, M., Geuens, G., Nuydens, R., Willebrords, R., and De Mey, J. (1981) Taxol induces the assembly of free microtubules in living cells and blocks the organizing capacity of the centrosomes and kinetochores. *Proc. Natl. Acad. Sci. U.S.A.* **78,** 5608–5612
9. Snyder, J. P., Nettles, J. H., Cornett, B., Downing, K. H., and Nogales, E. (2001) The binding conformation of taxol in $\beta$-tubulin: a model based on electron crystallographic density. *Proc. Natl. Acad. Sci. U.S.A.* **98,** 5312–5316
10. Lipton, R. B., Apfel, S. C., Dutcher, J. P., Rosenberg, R., Kaplan, J., Berger, A., Einzig, A. I., Wiernik, P., and Schaumburg, H. H. (1989) Taxol produces a predominantly sensory neuropathy. *Neurology* **39,** 368–373
11. Dina, O. A., Chen, X., Reichling, D., and Levine, J. D. (2001) Role of protein kinase C$\epsilon$ and protein kinase A in a model of paclitaxel-induced painful peripheral neuropathy in the rat. *Neuroscience* **108,** 507–515
12. Matsumoto, M., Inoue, M., Hald, A., Xie, W., and Ueda, H. (2006) Inhibition of paclitaxel-induced A-fiber hypersensitization by gabapentin. *J. Pharmacol. Exp. Ther.* **318,** 735–740
13. Xiao, W. H., and Bennett, G. J. (2008) Chemotherapy-evoked neuropathic pain: abnormal spontaneous discharge in A-fiber and C-fiber primary afferent neurons and its suppression by acetyl-L-carnitine. *Pain* **135,** 262–270
14. Chen, J., Balmaceda, C., Bruce, J. N., Sisti, M. B., Huang, M., Cheung, Y. K., McKhann, G. M., Goodman, R. R., and Fine, R. L. (2006) Tamoxifen paradoxically decreases paclitaxel deposition into cerebrospinal fluid of brain tumor patients. *J. Neurooncol.* **76,** 85–92
15. Cavaletti, G., Cavalletti, E., Oggioni, N., Sottani, C., Minoia, C., D'Incalci, M., Zucchetti, M., Marmiroli, P., and Tredici, G. (2000) Distribution of paclitaxel within the nervous system of the rat after repeated intravenous administration. *Neurotoxicology* **21,** 389–393
16. Coull, J. A., Boudreau, D., Bachand, K., Prescott, S. A., Nault, F., Sík, A., De Koninck, P., and De Koninck, Y. (2003) Trans-synaptic shift in anion gradient in spinal lamina I neurons as a mechanism of neuropathic pain. *Nature* **424,** 938–942
17. Zhou, H. Y., Chen, S. R., Byun, H. S., Chen, H., Li, L., Han, H. D., Lopez-Berestein, G., Sood, A. K., and Pan, H. L. (2012) *N*-Methyl-D-aspartate receptor- and calpain-mediated proteolytic cleavage of K+-$Cl^-$ cotransporter-2 impairs spinal chloride homeostasis in neuropathic pain. *J. Biol. Chem.* **287,** 33853–33864
18. Polomano, R. C., Mannes, A. J., Clark, U. S., and Bennett, G. J. (2001) A painful peripheral neuropathy in the rat produced by the chemotherapeutic drug, paclitaxel. *Pain* **94,** 293–304
19. Chen, S. R., and Pan, H. L. (2003) Up-regulation of spinal muscarinic receptors and increased antinociceptive effect of intrathecal muscarine in diabetic rats. *J. Pharmacol. Exp. Ther.* **307,** 676–681
20. Chaplan, S. R., Bach, F. W., Pogrel, J. W., Chung, J. M., and Yaksh, T. L. (1994) Quantitative assessment of tactile allodynia in the rat paw. *J. Neu-*

*rosci. Methods* **53,** 55–63
21. Pan, Y. Z., and Pan, H. L. (2004) Primary afferent stimulation differentially potentiates excitatory and inhibitory inputs to spinal lamina II outer and inner neurons. *J. Neurophysiol.* **91,** 2413–2421
22. Zhao, Y. L., Chen, S. R., Chen, H., and Pan, H. L. (2012) Chronic opioid potentiates presynaptic but impairs postsynaptic *N*-methyl-D-aspartic acid receptor activity in spinal cords: implications for opioid hyperalgesia and tolerance. *J. Biol. Chem.* **287,** 25073–25085
23. Li, D. P., Chen, S. R., Pan, Y. Z., Levey, A. I., and Pan, H. L. (2002) Role of presynaptic muscarinic and GABA(B) receptors in spinal glutamate release and cholinergic analgesia in rats. *J. Physiol.* **543,** 807–818
24. Chen, S. R., Zhou, H. Y., Byun, H. S., Chen, H., and Pan, H. L. (2014) Casein kinase II regulates NMDA receptor activity in spinal cords and pain hypersensitivity induced by nerve injury. *J. Pharmacol. Exp. Ther.* **350,** 301–312
25. Ye, Z. Y., Li, D. P., Byun, H. S., Li, L., and Pan, H. L. (2012) NKCC1 upregulation disrupts chloride homeostasis in the hypothalamus and increases neuronal activity-sympathetic drive in hypertension. *J. Neurosci.* **32,** 8560–8568
26. Yvon, A. M., Wadsworth, P., and Jordan, M. A. (1999) Taxol suppresses dynamics of individual microtubules in living human tumor cells. *Mol. Biol. Cell* **10,** 947–959
27. Holzinger, A. (2009) Jasplakinolide: an actin-specific reagent that promotes actin polymerization. *Methods Mol. Biol.* **586,** 71–87
28. Cramer, L. P. (1999) Role of actin-filament disassembly in lamellipodium protrusion in motile cells revealed using the drug jasplakinolide. *Curr. Biol.* **9,** 1095–1105
29. Liu, X., Kapoor, T. M., Chen, J. K., and Huse, M. (2013) Diacylglycerol promotes centrosome polarization in T cells via reciprocal localization of dynein and myosin II. *Proc. Natl. Acad. Sci. U.S.A.* **110,** 11976–11981
30. Valensin, S., Ghiron, C., Lamanna, C., Kremer, A., Rossi, M., Ferruzzi, P., Nievo, M., and Bakker, A. (2009) KIF11 inhibition for glioblastoma treatment: reason to hope or a struggle with the brain? *BMC Cancer* **9,** 196
31. Delpy, A., Allain, A. E., Meyrand, P., and Branchereau, P. (2008) NKCC1 cotransporter inactivation underlies embryonic development of chloride-mediated inhibition in mouse spinal motoneuron. *J. Physiol.* **586,** 1059–1075
32. Galan, A., and Cervero, F. (2005) Painful stimuli induce *in vivo* phosphorylation and membrane mobilization of mouse spinal cord NKCC1 cotransporter. *Neuroscience* **133,** 245–252
33. Zhang, L. L., Delpire, E., and Vardi, N. (2007) NKCC1 does not accumulate chloride in developing retinal neurons. *J. Neurophysiol.* **98,** 266–277
34. Hannaert, P., Alvarez-Guerra, M., Pirot, D., Nazaret, C., and Garay, R. P. (2002) Rat NKCC2/NKCC1 cotransporter selectivity for loop diuretic drugs. *Naunyn Schmiedebergs Arch. Pharmacol.* **365,** 193–199
35. Payne, J. A., Rivera, C., Voipio, J., and Kaila, K. (2003) Cation-chloride co-transporters in neuronal communication, development, and trauma. *Trends Neurosci.* **26,** 199–206
36. Price, T. J., Hargreaves, K. M., and Cervero, F. (2006) Protein expression and mRNA cellular distribution of the NKCC1 cotransporter in the dorsal root and trigeminal ganglia of the rat. *Brain Res.* **1112,** 146–158
37. Delpire, E., Lu, J., England, R., Dull, C., and Thorne, T. (1999) Deafness and imbalance associated with inactivation of the secretory Na-K-2Cl co-transporter. *Nat. Genet.* **22,** 192–195
38. Ikeda, K., Oshima, T., Hidaka, H., and Takasaka, T. (1997) Molecular and clinical implications of loop diuretic ototoxicity. *Hear Res.* **107,** 1–8
39. Heng, Y. W., Lim, H. H., Mina, T., Utomo, P., Zhong, S., Lim, C. T., and Koh, C. G. (2012) TPPP acts downstream of RhoA-ROCK-LIMK2 to regulate astral microtubule organization and spindle orientation. *J. Cell Sci.* **125,** 1579–1590
40. Bubb, M. R., Spector, I., Beyer, B. B., and Fosen, K. M. (2000) Effects of jasplakinolide on the kinetics of actin polymerization. An explanation for certain *in vivo* observations. *J. Biol. Chem.* **275,** 5163–5170
41. Loewen, M. E., Wang, Z., Eldstrom, J., Dehghani Zadeh, A., Khurana, A., Steele, D. F., and Fedida, D. (2009) Shared requirement for dynein function and intact microtubule cytoskeleton for normal surface expression of cardiac potassium channels. *Am. J. Physiol. Heart Circ. Physiol.* **296,** H71–H83
42. Shpetner, H. S., Paschal, B. M., and Vallee, R. B. (1988) Characterization of the microtubule-activated ATPase of brain cytoplasmic dynein (MAP 1C). *J. Cell Biol.* **107,** 1001–1009
43. Boehmerle, W., Splittgerber, U., Lazarus, M. B., McKenzie, K. M., Johnston, D. G., Austin, D. J., and Ehrlich, B. E. (2006) Paclitaxel induces calcium oscillations via an inositol 1,4,5-trisphosphate receptor and neuronal calcium sensor 1-dependent mechanism. *Proc. Natl. Acad. Sci. U.S.A.* **103,** 18356–18361
44. Mayer, T. U., Kapoor, T. M., Haggarty, S. J., King, R. W., Schreiber, S. L., and Mitchison, T. J. (1999) Small molecule inhibitor of mitotic spindle bipolarity identified in a phenotype-based screen. *Science* **286,** 971–974
45. Haque, S. A., Hasaka, T. P., Brooks, A. D., Lobanov, P. V., and Baas, P. W. (2004) Monastrol, a prototype anti-cancer drug that inhibits a mitotic kinesin, induces rapid bursts of axonal outgrowth from cultured postmitotic neurons. *Cell Motil. Cytoskeleton* **58,** 10–16
46. Yoon, S. Y., Choi, J. E., Huh, J. W., Hwang, O., Lee, H. S., Hong, H. N., and Kim, D. (2005) Monastrol, a selective inhibitor of the mitotic kinesin Eg5, induces a distinctive growth profile of dendrites and axons in primary cortical neuron cultures. *Cell Motil. Cytoskeleton* **60,** 181–190
47. Myers, K. A., and Baas, P. W. (2007) Kinesin-5 regulates the growth of the axon by acting as a brake on its microtubule array. *J. Cell Biol.* **178,** 1081–1091
48. Rosenmund, C., and Westbrook, G. L. (1993) Calcium-induced actin depolymerization reduces NMDA channel activity. *Neuron* **10,** 805–814
49. Reynolds, A., Parris, A., Evans, L. A., Lindqvist, S., Sharp, P., Lewis, M., Tighe, R., and Williams, M. R. (2007) Dynamic and differential regulation of NKCC1 by calcium and cAMP in the native human colonic epithelium. *J. Physiol.* **582,** 507–524
50. Collot, M., Louvard, D., and Singer, S. J. (1984) Lysosomes are associated with microtubules and not with intermediate filaments in cultured fibroblasts. *Proc. Natl. Acad. Sci. U.S.A.* **81,** 788–792
51. Jakab, R. L., Collaco, A. M., and Ameen, N. A. (2011) Physiological relevance of cell-specific distribution patterns of CFTR, NKCC1, NBCe1, and NHE3 along the crypt-villus axis in the intestine. *Am. J. Physiol. Gastrointest. Liver Physiol.* **300,** G82–G98
52. Matteoni, R., and Kreis, T. E. (1987) Translocation and clustering of endosomes and lysosomes depends on microtubules. *J. Cell Biol.* **105,** 1253–1265
53. Rodriguez, O. C., Schaefer, A. W., Mandato, C. A., Forscher, P., Bement, W. M., and Waterman-Storer, C. M. (2003) Conserved microtubule-actin interactions in cell movement and morphogenesis. *Nat. Cell Biol.* **5,** 599–609
54. Siegrist, S. E., and Doe, C. Q. (2007) Microtubule-induced cortical cell polarity. *Genes Dev.* **21,** 483–496
55. Sirajuddin, M., Rice, L. M., and Vale, R. D. (2014) Regulation of microtubule motors by tubulin isotypes and post-translational modifications. *Nat. Cell Biol.* **16,** 335–344
56. Kapitein, L. C., Schlager, M. A., Kuijpers, M., Wulf, P. S., van Spronsen, M., MacKintosh, F. C., and Hoogenraad, C. C. (2010) Mixed microtubules steer dynein-driven cargo transport into dendrites. *Curr. Biol.* **20,** 290–299
57. Zheng, Y., Wildonger, J., Ye, B., Zhang, Y., Kita, A., Younger, S. H., Zimmerman, S., Jan, L. Y., and Jan, Y. N. (2008) Dynein is required for polarized dendritic transport and uniform microtubule orientation in axons. *Nat. Cell Biol.* **10,** 1172–1180
58. Walter, W. J., Koonce, M. P., Brenner, B., and Steffen, W. (2012) Two independent switches regulate cytoplasmic dynein's processivity and directionality. *Proc. Natl. Acad. Sci. U.S.A.* **109,** 5289–5293
59. Choi, W. S., Khurana, A., Mathur, R., Viswanathan, V., Steele, D. F., and Fedida, D. (2005) Kv1.5 surface expression is modulated by retrograde trafficking of newly endocytosed channels by the dynein motor. *Circ. Res.* **97,** 363–371
60. Saunders, A. M., Powers, J., Strome, S., and Saxton, W. M. (2007) Kinesin-5 acts as a brake in anaphase spindle elongation. *Curr. Biol.* **17,** R453–R454